Thermochimica Acta 485 (2009) 33–42

Contents lists available at ScienceDirect

Thermochimica Acta

journal homepage: www.elsevier.com/locate/tca

Temperature- and moisture-dependent phase changes in crystal forms of barbituric acid

Neslihan Zencirci, Elisabeth Gstrein, Christoph Langes, Ulrich J. Griesser*

Institute of Pharmacy, Faculty of Chemistry and Pharmacy, University of Innsbruck, Innrain 52, 6020 Innsbruck, Austria

ARTICLE INFO

Article history:
Received 20 October 2008
Received in revised form
20 November 2008
Accepted 3 December 2008
Available online 11 December 2008

Keywords:
Barbituric acid
Hydrate
Crystal polymorphism
Moisture sorption
Dehydration
Thermal analysis
Solution calorimetry
Spectroscopy
Thermochemistry
X-ray powder diffraction

ABSTRACT

The dihydrate of barbituric acid (BAc) and its dehydration product, form II were investigated by means of moisture sorption analysis, hot-stage microscopy, differential scanning calorimetry, thermogravimetry, solution calorimetry, IR- and Raman-spectroscopy as well as powder X-ray diffraction. The dihydrate desolvates already at and below 50% relative humidity (RH) at 25 °C whereas form II is stable up to 80% RH, where it transforms back to the dihydrate. The thermal dehydration of barbituric acid dihydrate (BAc-H2) is a single step, nucleation controlled process. The peritectic reaction of the hydrate was measured at 77 °C and a transformation enthalpy of $\Delta_{trs}H_{H2\text{-}II} = 17.3\ kJ\ mol^{-1}$ was calculated for the interconversion between the hydrate and form II. An almost identical value of 17.0 kJ mol^{-1} was obtained from solution calorimetry in water as solvent ($\Delta_{sol}H_{H2} = 41.5$, $\Delta_{sol}H_{II} = 24.5\ kJ\ mol^{-1}$). Additionally a high-temperature form (HT-form) of BAc, which is enantiotropically related to form II and unstable at ambient conditions has been characterized. Furthermore, we observed that grinding of BAc with potassium bromide (KBr) induces a tautomeric change. Therefore, IR-spectra recorded with KBr-discs usually display a mixture of tautomers, whereas the IR-spectra of the pure trioxo-form of BAc are obtained if alternative preparation techniques are used.

1. Introduction

Barbituric acid [BAc, 2,4,6(1H,3H,5H)-pyrimidinetrione)] (Scheme 1) is the pharmacologically inactive lead structure of the 5,5-subsituted barbiturates, which have played an important role as sedative/hypnotic drugs in the first half of the 20th century but have now been replaced to a large extent by benzodiazepines and other drugs which provide less potential for abuse and are less toxic. Some of the derivatives are still therapeutically used (mainly as general anesthetics and anticonvulsants) while barbituric acid itself is used as precursor for the synthesis of a wide range of materials such as pigments [1], dyes [2], polymers [3] or the Vitamin B_2 (riboflavin) synthesis [4]. Since the synthesis of this compound in 1863 by Adolf von Baeyer (Nobel prize in chemistry 1905 [5,6]), barbituric acid has been the subject of many thousand research papers, which highlight the importance of this substance.

Our interest in this compound emerged from a broader study on the structure–property relationship of biologically active barbituric acid derivatives. Amazingly, only two crystal forms of BAc, an anhydrous form and a dihydrate, had been known until a few years ago (140 years after its first description!). In the last five years another polymorphic form of the dihydrate, a solvate and at least two additional (unsolvated) polymorphic forms have been discovered, which will be discussed in more detail below. This fact attests clearly that polymorphism has been widely disregarded in the past. However, since a sound knowledge of solid-state properties of used materials is regarded as a prerequisite in modern pharmaceutical and chemical industries [7–9] polymorphism and related phenomena have become a research topic that attracts a rising number of scientists today.

The dihydrate of barbituric acid (BAc-H2) was already described by Baeyer in 1863 and the crystal structure of this orthorhombic form was first determined by Jeffrey et al. in 1961 [10]. Two years later the crystal structure of the "anhydrous" BAc (monoclinic, $P2_1/n$) was reported by Bolton [11]. The structure shows hydrogen-bonded ribbons that pack in a herringbone like manner. In 2004 Lewis et al. [12] published the crystal structure of another monoclinic form ($P2_1/a$) with two independent molecules in the asymmetric unit (the Bolton form has just one), forming almost planar hydrogen-bonded sheets that stack with a distance of approximately 2.91 Å. The "Lewis form" (named form II) is the closer packed structure [12,13]. The density difference to the original "Bolton form" (named form I) is 6.3%, which is a rather high value for a pair of polymorphs (calculated densities from structure

* Corresponding author. Tel.: +43 512 507 5309; fax: +49 512 507 2939.
E-mail address: ulrich.griesser@uibk.ac.at (U.J. Griesser).

0040-6031/$ – see front matter © 2008 Elsevier B.V. All rights reserved.
doi:10.1016/j.tca.2008.12.001

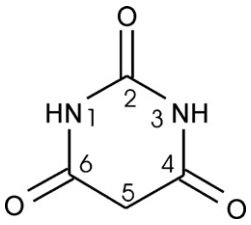

Scheme 1. Molecular formula of barbituric acid [2,4,6,(1H,3H,5H)-pyrimidinetrione].

determinations at 150 K [12]). This feature as well as lattice energy calculations, performed by the same authors, indicate that form II is the thermodynamically stable form. Braga et al. [14] noticed that commercial BAc (Aldrich) consists of pure form II and they verified with variable temperature X-ray powder diffraction experiments that thermal dehydration of BAc-H2 exclusively results in this form. Thus, it is clear that form II had been present since Baeyer's days and that without realizing it Bolton accidentally crystallized and measured the crystal structure of the metastable form I (kinetic form). Braga et al. [14] also obtained a new solid-state form by thermal treatment (200–250 °C) of BAc salts (ammonia, methylamine or dimethylamine). These authors mentioned that this "compound III" (also called "form III") "may well be a new polymorph" according to its IR- and ^{1}H NMR-spectra, but a clear evidence that this crystalline phase is actually a new polymorph of barbituric acid is missing. However, the existence of a new high-temperature phase has been reported recently by Roux et al. [15], which is consistent with our findings. This form (HT-form) occurs on heating form II to about 245 °C and in differential scanning calorimetry (DSC) experiments this transformation is indicated by an endothermic peak ($\Delta_{trs}H_{II\text{-}HT} = 1.3 \pm 0.04$ kJ mol^{-1}) occurring about 10 K below the melting process ($T_{fus,HT} = 526.4 \pm 0.5$, $\Delta_{fus}H_{HT} = 20.87 \pm 0.14$ kJ mol^{-1}). Indexing of the powder pattern resulted in a triclinic unit cell for the HT-form.

The structure of a 1:2 solvate BAc with dioxane was reported by Al-Saqqar et al. [16]. The interesting feature of this solvate is the lack of self-recognition of BAc molecules, i.e. strong hydrogen bonds are formed exclusively with solvent molecules but not with another BAc molecule. It is mentioned in this paper that this solvate is rather unstable, but there is no information so far which polymorph results after the desolvation process.

In a single crystal X-ray diffraction study Nichol and Clegg [17] noticed a reversible transformation (range: 200–220 K) between the orthorhombic dihydrate (*Pnma*) and a low temperature phase of the dihydrate, which was a non-merohedrically twinned and crystallized monoclinic space group ($P2_1/n$). The change involves mainly an out of plane displacement of the water molecules and the sp^3-hybridized C atom of BAc, but not the hydrogen bonding motif. The pyrimidinetrione-ring in the BAc molecule of the orthorhombic dihydrate (BAc-H2) is planar and forms an almost perfectly planar H-bonded networks (sheets) with water (see Section 3.5).

However, only little information is available in the literature on the thermal and moisture dependent stability of the orthorhombic dihydrate. In an early thermogravimetric analysis (TGA) study, Berlin et al. [18] reported that BAc-H2 dehydrates between 20 and 70 °C. Jeffrey et al. [10] stated that single crystals of BAc-H2 decomposed on the diffractometer during a data collection at room temperature. We have also noticed in Byrn's famous book on solid-state chemistry of drugs [19] a summary of a study on the moisture desolvation kinetics of BAc-H2 performed by P.R. Perrier 1980 (thesis, Purdue university, unpublished). These data show that the dihydrate is stable at 60% relative humidity (RH) but desolvates slowly at 33% RH. The desolvation rate increases strongly towards lower RH conditions. Furthermore, it was observed in this study that the dehydration of small crystals can be described by a zero-order kinetic model, whereas the dehydration process of larger crystals follows the well known Avrami–Erofe'ev equation ($n = 1/4$). Thus, it becomes evident that the BAc dihydrate is a rather unstable stoichiometric hydrate that may easily desolvate during handling and storage, similar to the hydrates of caffeine [20] and theophylline [21].

In spite of the extensive literature about BAc, there are still open questions and several information gaps regarding the solid-state behaviour of the different forms including a lack of thermoanalytical data. The main interest of our study was focused towards the thermal and moisture dependent phase change between the dihydrate and form II, since these two forms are those of highest practical relevance. For compounds forming a hydrate, the knowledge of the equilibrium moisture sorption/desorption isotherm is regarded as a key information for issues related to handling and storage, but such data are also useful for the experimental setup and interpretation of thermoanalytical data. Therefore, we employed gravimetric moisture sorption and moisture stage microscopy experiments along with hot-stage microscopy, differential scanning calorimetry, thermogravimetry, IR- and Raman-spectroscopy as well as X-Ray powder diffraction in the present study. In the course of our work we also observed and characterized the transformation of form II to the HT-form, which has been described very recently by Roux et al. [15]. An aim of our study was also to clarify the relations and interconversions between the different crystal forms of BAc and to connect the pieces of information to a clearer view about the polymorphism of this popular compound.

2. Experimental

2.1. Materials and preparation of the forms

Barbituric acid (puriss. p.a. >99.5%, Fluka) was purchased from Sigma–Aldrich Inc. (Steinheim, D) and consists of pure form II. This form was also obtained by dehydration of the freshly crystallized dihydrate at room condition. Samples of the HT-form were produced by heating form II to 248 °C in a DSC pan and subsequent quench cooling (withdrawal of the hot pan). Pure samples of the HT-form (no seeds of form II) produced in this way were found to be stable for at least 24 h at room temperature, whereas traces of form II increase the retransformation rate significantly.

Samples of the dihydrate were produced by crystallization from water/ethanol. A solution of barbituric acid in this solvent mixture was allowed to slowly evaporate under ambient conditions. The obtained crystals were stored in a desiccator at 75% relative humidity (saturated sodium chloride solution) at 25 °C to prevent dehydration.

In order to obtain form I we performed a few solvent crystallization experiments (at 20 and 8 °C) according to the instructions of Lewis et al. [12]. However, evaporation experiments from different solvents (acetonitrile, 1-propanol, ethanol) or the addition of an antisolvent (diethylether or chloroform) to a solution of BAc in acetonitrile, ethanol or methanol resulted either in form II or mixtures of forms I and II. We noticed that crystals of the kinetic form I grow in the solution but quickly transform to the stable form II. We thus failed to produce a sample of form I which is sufficiently pure to determine reliable thermochemical data.

All solvents used in this study were of analytical grade (Merck, Darmstadt, D).

2.2. Polarized light and hot-stage light microscopy (HSM)

An Olympus BH2 polarization microscope (Olympus Optical GmbH, Vienna, A) equipped with a Kofler hot-stage (Reichert Thermovar, Vienna, A) was used for optical and hot-stage microscopic

observations. The BAc-H2 samples were either prepared as a dry preparation (glass slide plus cover slip) or as a suspension in silicon oil. Variable heating rates were applied between 4 and 20 K min^{-1}.

2.3. Optical microscopy with humidity stage

For optical microscopic observations under controlled temperature and humidity conditions a VGI2000 M stage (Vapor Generator Instrument, Surface Measurement Systems Ltd, London, UK) mounted on an Olympus BH2 polarization microscope (Olympus Optical GmbH, Vienna, A) was used. The dehydration process of BAc-H2 was performed at 25 °C and 30% relative humidity and the images were recorded with an Olympus ColorView IIIu digital camera using the cell D software (Soft Imaging System, Hamburg, D).

2.4. Fourier transform infrared (FT-IR) spectroscopy

FT-IR-spectra were recorded with a Bruker IFS 25 spectrometer connected with the IR microscope I (Bruker Analytische Messtechnik GmbH, Karlsruhe, D). The samples were prepared on ZnSe discs and measured in transmission mode (15× Cassegrain-objective, spectral range 4000–600 cm^{-1}, resolution 4 cm^{-1}, 64 interferograms per spectrum).

Potassium bromide (KBr) discs (13 mm) were prepared by gently grinding and mixing 0.5 mg BAc with 200 mg KBr in a mortar with pestle, evacuating of the mixture in the pressing tool for 30 s (~10 mbar) and applying a pressure of about 800 MPa for about 1 min using an hydraulic press. The spectra were recorded in the range of 4000–400 cm^{-1} at an instrument resolution of 2 cm^{-1} (64 scans per spectrum). In order to study the interactions of BAc with KBr during mechanical treatment, a mixture of form II with KBr (50/50 ratio) was ground in a 10 mL grinding jar (stainless steel, 10 mm balls) using a ball mill (Retsch Schwingmühle MM301, Haan, D) for 30 min (frequency: 30 Hz s^{-1}). The sample was measured on a ZnSe disk.

2.5. Fourier transform Raman (FT-Raman) spectroscopy

FT-Raman spectra were recorded on a Bruker RFS 100 Raman-spectrometer (Bruker Analytische Messtechnik GmbH, Ettlingen, D), equipped with a Nd:YAG laser (1064 nm) as the excitation source and a liquid-nitrogen-cooled, high sensitivity Ge-detector. The barbituric acid dihydrate was measured in a small glass tube and form II in an aluminium pan. The spectra were recorded with a laser power of 200 mW (64 scans per spectrum) at a resolution of 4 cm^{-1}.

2.6. Powder X-ray diffractometry (PXRD)

The X-ray powder diffraction patterns (XRPD) were obtained with a X'Pert PRO diffractometer (PANalytical, Almelo, NL) equipped with a theta/theta coupled goniometer in transmission geometry, programmable *XYZ* stage with well plate holder, Cu $K\alpha_{1,2}$ radiation source (wavelength 0.15419 nm) with a focussing mirror, a 0.5° divergence slit and a 0.02° soller slit collimator on the incident beam side, a 2 mm antiscattering slit and a 0.02° soller slit collimator on the diffracted beam side and a solid-state PIXcel detector. The samples were prepared on a 3 μm Mylar foil and recorded at a tube voltage of 40 kV and tube current of 40 mA, applying a step size of 0.013° 2θ in the angular range of 2°–40° 2θ with 40 s per step.

The pattern of the HT-form used for indexing was recorded (25 °C, 40% RH) in the angular range of 2–60° 2θ with a step size of 0.013° and 60 s per step. Peak positions for the unit cell determination were obtained by profile fitting using High Score Plus [22], and indexing of the reflections was performed with the Crysfire suite [23] in combination with Chekcell [24]. The LeBail-refinement was also performed with the program High Score Plus [22] using the starting values for the unit cell metric from the Crysfire indexing results. Pseudo-Voigt functions were utilized to describe the peak shape. The background was modeled by linear interpolation between points with no or low Bragg intensity contribution. A graphical comparison between the observed and calculated powder patterns is given in Fig. S3 (supplementary material).

2.7. Thermogravimetric analysis

A TGA 7 system (Perkin–Elmer, Norwalk, CT, USA) was used for thermogravimetric measurements. Samples (2–6 mg) were placed into 50 μl platin pans and the determinations were carried out under a nitrogen purge (balance purge: 50 mL min^{-1}, sample purge: 25 mL min^{-1}). The temperature calibration was performed with alumel and nickel (Curie-point standards, Perkin–Elmer) and the calibration of the electrobalance with a 100 mg reference weight (Perkin–Elmer) according to the manufacturers instructions.

2.8. Differential scanning calorimetry

DSC thermograms were recorded on a DSC 7 (Perkin–Elmer, Norwalk, CT, USA), operated with the Pyris 2.0 software. Samples of approximately 1–3 mg were accurately weighed (±0.0005 mg) using a UM3 ultramicrobalance (Mettler, Greifensee, CH) into sealed or pinholed Al-pans (30 μL). The samples were scanned through the range of 25–270 °C at different heating rates between 2 and 10 K min^{-1}, with dry nitrogen as purge gas (purge: 20 mL min^{-1}). The instrument was calibrated for temperature with pure benzophenone (m.p. 48.0 °C) and caffeine (m.p. 236.2 °C), and the energy calibration was performed with pure indium (purity 99.999%, m.p. 156.6 °C, heat of fusion 28.45 J g^{-1}). The errors of the stated temperatures (extrapolated onset temperatures) and enthalpy values (Table 1) are calculated at 95% confidence intervals (CI) based on at least five measurements.

2.9. Solution calorimetry (SolCal) and RH-perfusion experiments

The enthalpies of solution ($\Delta_{sol}H$) of the hydrate and form II were measured with the precision solution calorimeter of the TAM III Thermal Activity Monitor (TA Instruments Inc.). The measurement temperature was 25 ± 10^{-4} °C, the volume of the vessel 100 mL and the stirrer speed 500 rpm. Three measurements with sample amounts of approximately 100 mg (accuracy ±0.0005 mg) were performed per solid form. The calorimeter was calibrated with KCl (analytic grade, >99.5%, Merck) – standard solution enthalpy $\Delta_{sol}H^{\circ} = 17.51 \pm 0.0016$ kJ mol^{-1} in good agreement with the established NIST value of $\Delta_{sol}H^{\circ} = 17.584 \pm 0.017$ kJ mol^{-1} [25]. The TAM Assistant software v 1.2 was used for the data analysis.

RH perfusion calorimetry experiments were performed with the TAM III nanocalorimeter unit in a 4 mL stainless steel RH perfusion ampoule. Only one measurement with a sample amount of 22 mg (accuracy ±0.0005 mg) was performed. The relative humidity was controlled with two mass flow controllers and the following measurement profile was executed: 60, 65, 70, 75, 78, 80, 82, 84, 86, 88 and 90% RH. Dry N_2 was used as the carrier gas at a constant flow rate of 100 mL h^{-1}. The RH perfusion cell was calibrated with saturated solutions of NaCl (75.3% RH), $Mg(NO_3)_2$ (52.8% RH) and LiCl (11.3% RH). The heat flow of the empty RH perfusion ampoule (baseline run) was subtracted from the heat flow of the sample measurement.

2.10. Dynamic moisture sorption analysis (SPS11)

Dynamic moisture sorption and desorption were determined gravimetrically at 25 °C using an automatic multi-sample moisture

Table 1
Physicochemical data for barbituric acid polymorphs.

Form	HT	II	H2
T_{fus} (°C)	253 (HSM)		
DSC (onset)	252.7 ± 0.5	$<T_{fus,HT}$	
$\Delta_{fus}H$ (kJ mol^{-1})	20.33 ± 0.21	21.66[a]	
$\Delta_{fus}S$ (J mol^{-1} K^{-1})	38.7	–	
T_{trs} exp. (°C)			
DSC-studies (onset)		239.9 ± 0.5 (II → HT)	
HSM studies		242–245	
$\Delta_{trs}H$ (kJ mol^{-1})		1.33 ± 0.04 (II → HT)	17.3 (H2 → II, DSC) 17.03 (H2 → II, SolCal) −17.00 (II → H2, RH perf.)
$\Delta_{diss}H_{H2\text{-}II}$ (kJ mol^{-1}) at T_{diss} (closed DSC pan)			22.40 ± 0.18 (H2 → II)
$T_{diss,\ H2}$ (°C), DSC (onset)			76.8 ± 0.2 (H2 → II)
$\Delta_{dehy}H_{H2\text{-}II}$ (kJ mol^{-1}) at $T < T_{diss}$ (open DSC pan)			101.79 ± 2.28 (H2 → II)
$\Delta_{sol}H$ in water at 25 °C (kJ mol^{-1})		24.51 ± 0.17	41.54 ± 0.75
d_{calc} (g cm^{-3}) at (°C)		1.723 (−123)[b]	1.548 (−3)[c]
Selected IR-bands (cm^{-1})			
νNH	3237, 3107	3204, 3097	3215, 3073
νC=O	1748, 1707	1752, 1707, 1694	1707
νOH			3529, 3487, 3454, 3380
δOH_2			1615
νNH out of plane	799	806	794
Selected Raman-bands (cm^{-1})			
νNH	3232, 3115	3202, 3083	3203, 3076
νC—H_2	2980, 2893	2915, 2877	2962, 2925
νC=O	1730, 1695	1732, 1719, 1700	1732, 1715, 1688
νCN	1241, 1193	1252, 1191	1259, 1201
Ring breathing	662	663	668
$\delta_{ring\ bending}$	506, 469	507, 476	511, 497
δC=O bending	397	402	411

T_{fus}: melting point; T_{trs}: transition temperature; $\Delta_{fus}H$: heat of fusion; $\Delta_{trs}H$: transition enthalpy; T_{diss} and $\Delta_{diss}H$: temperature and heat of dissociation of H2; $\Delta_{dehy}H$: heat of dehydration; SolCal: solution calorimetry; RH perf.: RH perfusion cell, isothermal calorimetry. All errors are stated as the confidence interval (CI) at the 95% level.

[a] Calculated: sum of $\Delta_{fus}H_{HT}$ and $\Delta_{trs}H_{II\text{-}HT}$.

[b] Value taken from ref. [12].

[c] Value taken from ref. [17].

sorption analyzer (SPS11, Project-Meßtechnik, Ulm, D). Approximately 1.0 g of accurately weighed crystals (balance resolution: 10 μg) were placed in an aluminium sample dish (diameter: 5 cm), transferred into the sample compartment of the moisture sorption analyzer, and equilibrated at 40% RH. The RH was cycled in 10% steps down to 0% and up to 90% RH and down to 0% RH again. The mass change of the material was recorded every 7 min with the equilibrium condition set to band width <0.001% within 49 min, with the minimum residence time 60 min and the maximum residence time to 24 h for each RH level. When the equilibrium condition was fulfilled or the maximum residence time exceeded, the relative humidity was automatically changed to the next step. The mass change at equilibrium condition or at the time limit at each RH step was used to establish the moisture sorption isotherms.

3. Results and discussion

Table 1 summarizes the most important data from the literature and our own measurements of the two polymorphs and the dihydrate of barbituric acid and they are discussed in detail below.

3.1. Moisture sorption/desorption studies

The moisture sorption/desorption isotherm of barbituric acid (started with form II) and the optical appearance of a dehydrating single crystal of the dihydrate recorded at 30% RH (25 °C) are shown in Figs. 1 and 2. The sorption isotherm shows that the anhydrous form is stable (no water uptake) up to 70% RH. At higher moisture conditions the sample takes up water and the transformation to the hydrate occurs. The determined mass gain of 28.1% corresponds

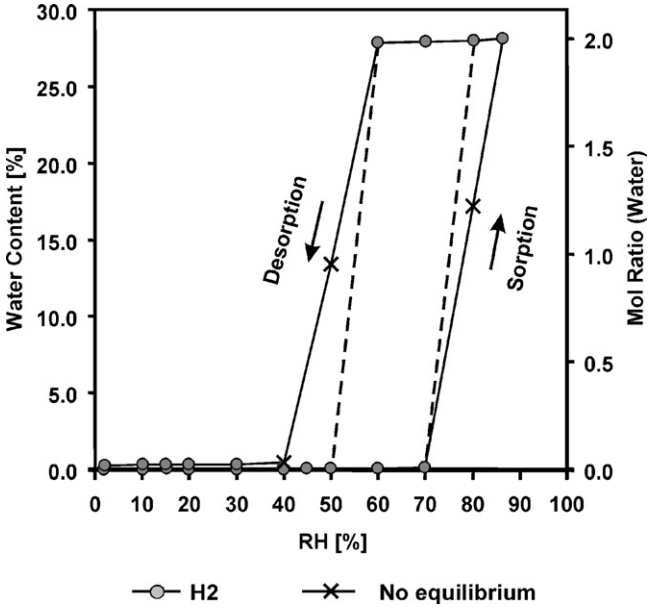

Fig. 1. Moisture sorption and desorption curves of barbituric acid (form II ↔ H2) at 25 °C. The circles represent data points that fulfil the preset equilibrium condition (mass change), whereas crosses mark measurement values that did not reach this requirement within the maximum equilibration time (set at 24 h). The dashed line indicates the course of the isotherm at the experimental equilibrium conditions.

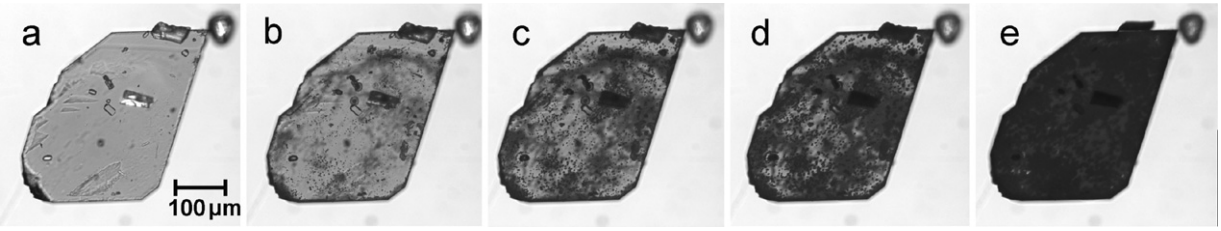

Fig. 2. Photomicrographs (a–e) of the dehydration process of BAc-H2 at 30% RH, 25 °C (moisture stage, <3 h). The occurrence of the dark spots and edges suggests a nucleation and growth mechanism that initiates at the surface of the crystal.

exactly to the theoretical value of 2 moles of water (28.13%). On decreasing the humidity, the dehydration to form II occurs already at 50% RH. The clear steps and the hysteresis loop between the sorption and desorption isotherm is characteristic for stoichiometric hydrates. However, it becomes obvious from this observation that BAc-H2 represents a rather unstable hydrate, which loses its water at common ambient conditions (below 50% RH) rather fast. This information is crucial for the handling of the dihydrate and therefore all experiments in the present study were carried out with hydrate samples that have been stored at 75% RH.

The optical changes (transmission light microscopy) of the dehydration process at 30% RH (25 °C) are shown in Fig. 2. Obviously, the reaction starts at the crystal surface where a number of separated nuclei occur (black spots and black edges). The quantity of these nucleation centres remains constant during the dehydration process, while they expand slowly. This confirms that the desolvation follows a nucleation and growth mechanism, as observed by Byrn et al. [19]. The process results in particles of the original shape of the hydrate that consist of small crystallites of form II (pseudomorphosis). The crystals appear microscopically opaque because of light scattering effects at the many surfaces in such multi-particle assemblies. An exposure of the same sample to 75% RH for 35 hours results in the dihydrate again. This process is optically not observable in the opaque particles, but was confirmed by IR-micro-spectroscopy.

3.2. Thermal analysis

3.2.1. Hot-stage micrcoscopic observations

Crystals of the thermodynamically stable form II sublimates strongly above 170 °C to highly birefringent grains and prisms. At about 240 °C a solid–solid transformation (form II to the HT-form) can be observed (Fig. 3), which can be recognized mainly due to the changes in interference colours of the crystals. The high-temperature form melts then at 253 °C to give an initially clear melt, which starts to decompose a few Kelvin above the melting point. The decomposition can be recognized by the formation of bubbles, brown colouring of the melt and the sudden formation of tiny crystals of a decomposition product (see supplementary material, Fig. S4).

Depending on the crystallization condition, the morphology of the orthorhombic crystals of BAc-H2 may vary. As the crystals are not stable on exposure to air (<60% RH) the hot-stage microscopy experiments were performed with freshly prepared single crystals.

The dehydration process of BAc-H2 in a preparation of low viscous silicon oil (1000 mPa s, 25 °C) and a low heating rate (5 K min^{-1}) is shown in Fig. 4A. The desolvation starts already at 30 °C, which is indicated by spots emerging at the surface of the crystals. These spots represent the nucleation centres of form II. The number of such nucleation centres increase with increasing temperature and the process results in only very small crystals (dimension of a few μm). From this behaviour it is obvious that the desolvation process is controlled by a nucleation and growth mechanism involving a high nucleation rate but a low growth rate. The process yields aggregates of rather homogeneously sized crystals of form II while the original shape of the hydrate crystals is maintained. This process, called "pseudomorphosis", is characteristic for stoichiometric hydrates. However, freshly crystallized hydrate crystals embedded in a silicon oil with higher viscosity (1,000,000 mPa s, 25 °C) and heated at higher rates (~10 K min^{-1}) show a different behaviour. As shown in Fig. 4B only a few, fast growing crystals of the anhydrous phase nucleate at 77 °C at the surface of original hydrate crystal. The crystals are surrounded by a court, which represents the reaction zone with the highest mobility where BAc molecules must diffuse towards the growing anhydrate phase (form II). This behaviour is a characteristic feature of a so-called inhomogeneous (or incongruent) melting process where the hydrate undergoes partial fusion whereas at the same time the melt decomposes to a lower hydrate or an anhydrous form and water. As for BAc-H2, one cannot clearly observe a melt if the nucleation and growth of the anhydrous phase is very high. The incongruent melting process of a hydrate starts at a temperature, which is a physical constant and is commonly referred to as peritectic temperature (the dissociation process of the hydrate at this temperature is also called peritectic decomposition). The peritectic temperature for BAc-H2 is 77 °C, which means that the hydrate cannot exist above this temperature (referred to normal pressure). The release of water in the oil is visible by the formation of bubbles. Because of the fast crystal growth, irregular junks of form II emerge during this process. Further heating to about 110 °C shows a darkening of the mostly rectangular particles, which occupy less volume than the original hydrate crystal due to the higher density of form II. As such desolvation reaction often result in some disorder and defect crystals, we assume that the observed darkening, which indicates the formation of small crystal domains due to a shrinking and crack formation, can be explained by thermal relaxation effects at elevated temperature and the release of traces of residual water.

3.3. DSC/TGA and solution calorimetry

Representative DSC curves of forms II and H2 of BAc and the TGA curve of the dihydrate are illustrated in Fig. 5. Key data of the thermal analytical investigations are summarized along with other results in Table 1. All desolvation experiments of the dihydrate resulted in form II of BAc, which was confirmed by IR-spectroscopy and/or PXRD.

TGA of the BAc-H2 (Fig. 5, curve 5) shows a one step loss of water. We measured a mass loss of 22.33 ± 0.04% (w/w) between 25 and 90 °C corresponding to 2.05 moles equivalent water (theoretical value for 2 moles water is 21.95%).

The DSC curve of form II (Fig. 5, curve 1) shows an endothermic transformation process at 240 °C to the HT-form, which melts at 253 °C under weak decomposition. A narrow range of only 3 °C (238–241 °C) was observed for the transition temperature at different heating rates (2.5–40 K min^{-1}), which is indicative for a rather high activation energy for this solid–solid transition. The measured heat of transition ($\Delta_{trs}H_{II\text{-}HT}$ = 1.33 kJ mol^{-1}) and heat of fusion ($\Delta_{fus}H_{HT}$ = 20.33 kJ mol^{-1}) match very well with the values of 1.30 and 20.87 kJ mol^{-1} reported by Roux et al. [15]. The fact that the

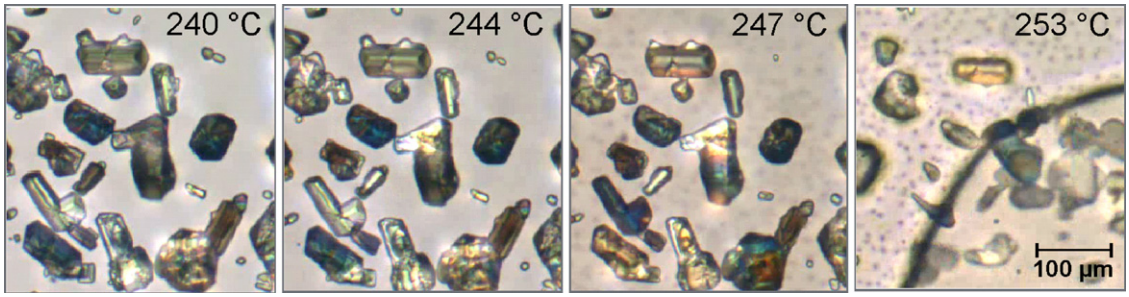

Fig. 3. Photomicrographs showing the transformation of BAc form II (sublimates, prepared in silicon oil) to the HT-form on heating (indicated by the change of interference colours or brightness of the crystals) and the start of the melting process at 253 °C (polarized light, angle of the analyzer about 30 ° from transmission axes).

transition is endothermic, indicates that form II and the HT-form are enantiotropically related (heat of transition rule [26]), which implies that the transformation is in principle reversible in the solid state. We therefore performed several heating cooling cycles at different heating rates. As shown in Fig. 6 (cycle A, rate 10 K min^{-1}) an exothermic peak occurs in the cooling curve at around 75 °C, confirming that the transformation is indeed reversible. This is also supported by the observation that the evolved heat in this process shows about the same magnitude as the heat of transition in the heating cycles and additionally by the recurring transformation to the HT-form (second heating cycle, curve 3). However, we noticed that the transformation to form II often does not occur in such a nar-

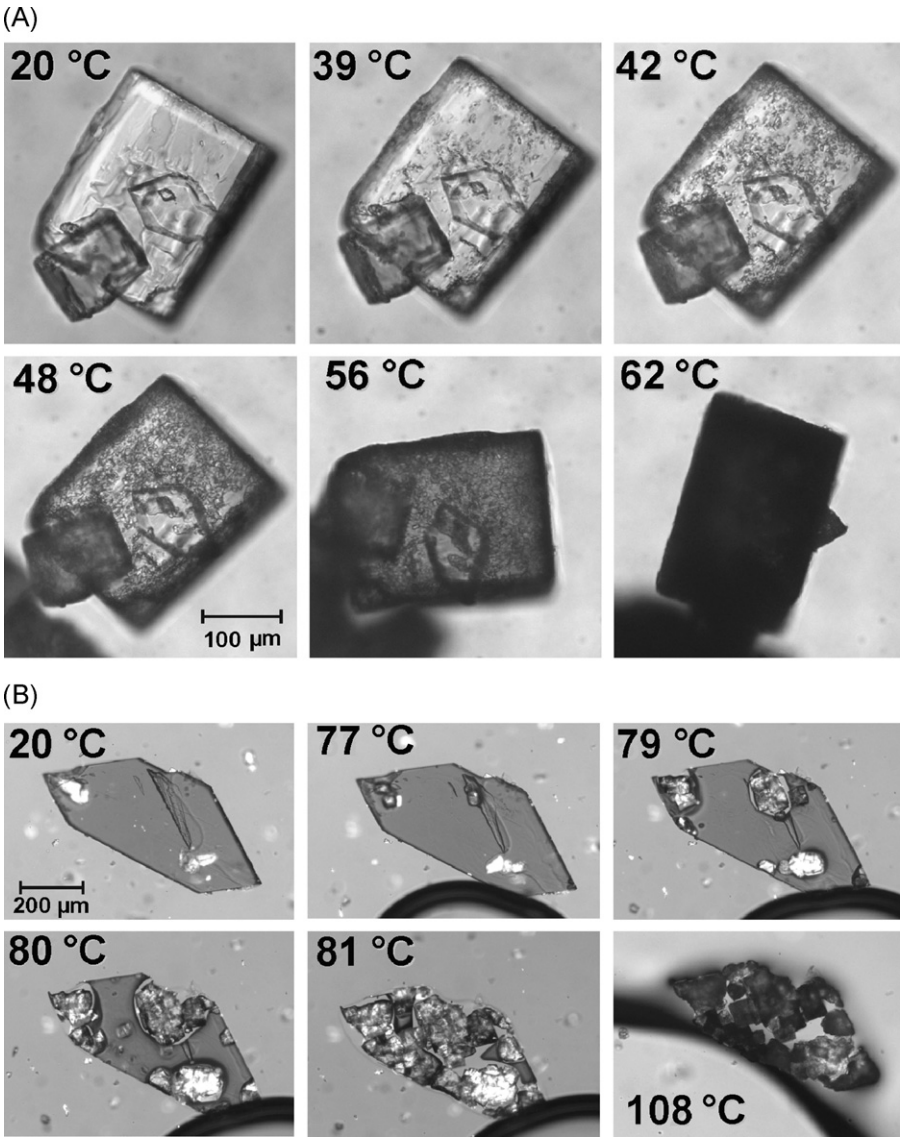

Fig. 4. Photomicrographs of the dehydration process of BAc-H2. Series A: process below the peritectic temperature (heated in a low viscous silicon oil) showing a high nucleation rate of form II and a characteristic pseudomorphosis (see text). Note that the shape of the original hydrate crystals is maintained. The black particle of the last picture (62 °C) turned out of the original position, why it appears smaller. Series B: preparation in a silicon oil with high viscosity showing the inhomogeneous melting process of BAc-H2 to form II on passing the peritectic temperature of 77 °C.

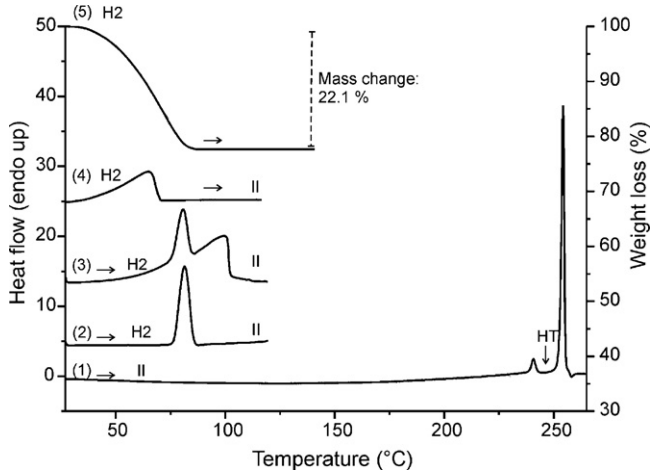

Fig. 5. DSC- and TGA-thermograms of (1) barbituric acid form II obtained by dehydration of BAc-H2; of BAc-H2 in (2) sealed pan with 10 K min^{-1} showing the peritectic decomposition peak, (3) pinholed pan with 10 K min^{-1} showing the peritectic peak and the evaporation peak of water, (4) pinholed pan 2.5 K min^{-1} where only the dehydration endotherm can be observed, and (5) TGA thermogram (10 K min^{-1}).

row temperature range. The cycle B in Fig. 6 shows an experiment with a lower cooling/heating rate (5 K min^{-1}) where the transformation to the stable form II is not visible as a unique peak but occurs over a wide temperature range during the cooling and heating cycle (curves 2 and 3 of cycle B). Microscopy experiments confirmed that the retransformation in slow cooling experiments takes place over wide temperature range. The endothermic transformation at 240 °C in the second heating cycle indicates that form II has been formed again. In the second heating run the transition of form II to the HT-form shifts slightly (2–3 K) to higher temperature. Furthermore the thermal stress in such repeated heating–cooling cycles produces more decomposition product so that stronger exothermic signals appear after the melting peak of the HT-form (curve C in Fig. 6).

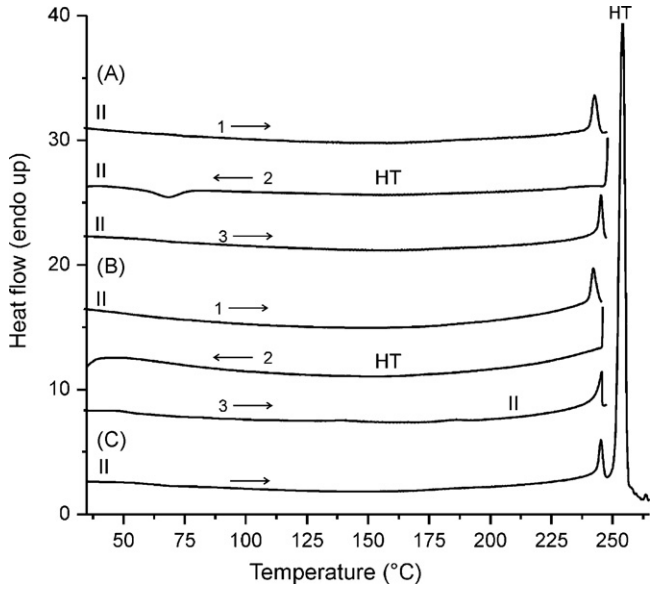

Fig. 6. DSC curves of form II at different heating/cooling programs. Right arrows mark heating and left arrows cooling programs. (A) Heating rate of 10 K min^{-1} shows a clear exothermic peak in the cooling curve for the back transformation of the HT-form to form II; (B) at a lower rate of 5 K min^{-1} the transition becomes diffuse and occurs over a wider temperature range and (C) heating curve of form II at 10 K min^{-1} shows the transition of form II to the HT-form followed by the melting peak.

DSC measurements of BAc-H2 were carried out in sealed and pinholed aluminium pans at different heating rates in order to verify the impact of the atmospheric conditions on the dehydration behaviour and to identify the involved processes. In a sealed pan (isochoric conditions, composition of the binary system remains unchanged) only one endothermic peak with an onset temperature of 77 °C is observed (curve 2 in Fig. 5). This process can be attributed to the peritectic decomposition (dissociation) of the dihydrate to form II ($\Delta_{diss}H_{H2\text{-}II}$ = 22.4 kJ mol^{-1}).

In a pinholed pan the desolvation process (indicated by the ascending baseline from about 50 °C) and the rather sharp peritectic decomposition of the hydrate, followed by the evaporation signal of water, can be identified (curve 3 in Fig. 5). The peritectic peak is also observed at a heating rate of 5 K min^{-1}, but at 2.5 K min^{-1} only a broad, plain dehydration process (curve 4 in Fig. 5) is recorded anymore. This desolvation process ($H2_{(s)} \rightarrow II_{(s)} + 2H_2O_{(g)}$) below the peritectic temperature (~30 to 70 °C) is connected with a high nucleation rate of form II, which can be derived from the microscopic observations (Fig. 4). The dehydration in the open DSC system requires much more energy ($\Delta_{dehy}H_{H2\text{-}II}$ = 101.8 kJ mol^{-1}) than the dissociation of the hydrate in the sealed pan, because the most of the heat is consumed by the vaporization process of the 2 moles water. If we apply Hess's law and subtract the known enthalpy value for the vaporization of water at the desolvation temperature (peak maximum, $T_{dehy} \approx 65$ °C, $\Delta_{vap}H^{\circ}_{H_2O}$ = 42.26 kJ mol^{-1} [27]) from the measured heat of dehydration according to Eq. (1), we get an estimation of the heat change upon hydrate formation from form II.

$$\Delta_{trs}H_{H2\text{-}II} = 2\Delta_{vap}H_{H_2O} - \Delta_{dehy}H_{H2\text{-}II} \quad (1)$$

The calculated enthalpy of this reaction is 17.3 kJ mol^{-1}. The transition enthalpy of the hydrate formation can also be obtained from the differences of the heats of solution $\Delta_{sol}H$ (Eq. (2)), as demonstrated elsewhere (e.g. [28]).

$$\Delta_{trs}H_{H2\text{-}II} = \Delta_{sol}H_{H2} - \Delta_{sol}H_{II} \quad (2)$$

This calculation (heat of solution values see Table 1) gives 17.03 kJ mol^{-1} and is in very good agreement with the value calculated from the DSC data. We also measured the transformation of form II to the hydrate by isothermal calorimetry using a controlled RH-perfusion cell (T = 25 °C). The integration of the exothermic heat flow peak (see Fig. S2, supplementary material) resulted in a reaction enthalpy for the hydrate formation of $\Delta_{hy}H_{II\text{-}H2}$ = −104.98 kJ mol^{-1}. Since the magnitude of the heat of condensation (exothermic process) of water is equal to the heat of vaporization (endothermic process) we can use Eq. (1) to calculate the transition enthalpy of form II to the dihydrate. Using a value of $\Delta_{vap}H^{\circ}_{H_2O}$ (25 °C) = 43.99 kJ mol^{-1} = $\Delta_{cond}H^{\circ}_{H_2O}$ (25 °C) [27] gives a transition enthalpy of $\Delta_{trs}H_{II\text{-}H2}$ = −17.00 kJ mol^{-1} which is also in good agreement with the values obtained from DSC and solution calorimetry experiments.

The difference between the transition enthalpies (H2 → II) and the dissociation enthalpy of the hydrate at the peritectic temperature in a sealed pan (22.4 kJ mol^{-1}) is about 5 kJ mol^{-1}. The fact that the latter value is higher than the calculated $\Delta_{trs}H_{H2\text{-}II}$ is not surprising considering that a part of the form II dissolves in the released water. From the enthalpy of solution of form II (24.51 kJ mol^{-1}) we can estimate that roughly 20% of BAc dissolves in the available amount of water at the peritectic temperature (~77 °C).

3.4. Fourier transform FT-IR and FT-Raman spectroscopy

The FT-IR and Raman spectra of the hydrated and the anhydrous forms (II and HT) are shown in Fig. 7 and the frequencies of some characteristic bands and Raman shifts are given in Table 1. The spec-

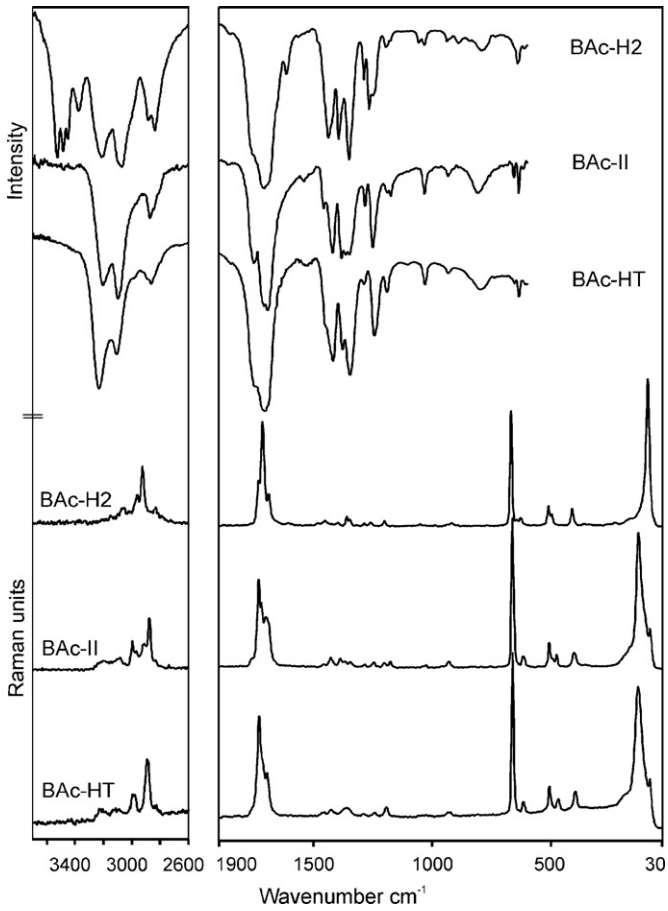

Fig. 7. FT-IR (top) and FT-Raman spectra (bottom) of barbituric acid form II (BAc-II), the dihydrate (BAc-H2) and the high-temperature form (BAc-HT).

tra of the two polymorphs and the hydrate show clear differences over almost the entire frequency range. An alteration of the hydrogen bond interactions between the –NH and –C=O groups in the two polymorphs (form II and HT) are indicated by changes of the NH vibrations around 3200 cm^{-1} and the C=O vibrations around 1700 cm^{-1}. From the hypsochromic shifts of the N—H stretching vibrations in the spectrum of the HT-form compared to form II (see Table 1) we can infer that the hydrogen bonds are slightly weaker in the HT-form. In addition to the two NH stretch vibrations the dihydrate shows four OH stretch bands of the two symmetry independent water molecules between 3600 and 3400 cm^{-1}, due to four different hydrogen bonds in the crystal structure (see Fig. 10 and refs. [10] and [17]). Furthermore, the dihydrate shows also the characteristic δOH_2 band of water at 1615 cm^{-1}.

Recently published IR-spectra of anhydrous forms of BAc prepared and recorded as KBr-discs [14] show additional clear absorption bands around 3500 cm^{-1} which however do not appear in our spectra. We therefore have performed a series of experiments which have clearly shown that mechanical treatment of the pure substance alone does not result in a different spectrum. By contrast, from analogous experiments in the presence of KBr we reproducibly obtained spectra with the bands at 3500 cm^{-1}, which additionally displayed clear changes in other spectral ranges. A comparison of the spectra obtained from a preparation of form II on a ZnSe disc without KBr and preparations together with the halide salt are shown in Fig. 8. From the bands at high wavenumbers (broader double band with maxima at 3562 and 3538 cm^{-1} and a single band at 3478 cm^{-1}), we postulate that the stable trioxo-tautomer partially transformed to an enol-tautomer. Further signs

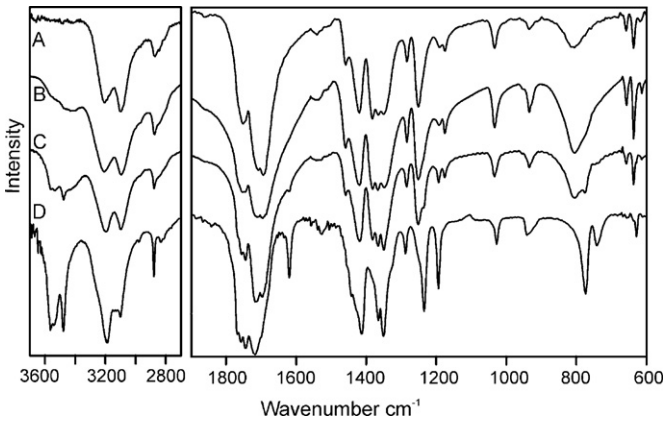

Fig. 8. FT-IR-spectra of BAc form II (A) flat sample preparation on a ZnSe disc (IR-microscope, transmission), (B) gently mixed and ground with KBr with pestle and mortar and pressed to a 13 mm pellet, (C) strongly ground with KBr (pestle and mortar, 13 mm pellet), (D) 1:1 mixture of BAc II and KBr ground for 30 min with a ball mill, prepared and recorded on ZnSe like sample (A).

for such a reaction are the changes in the relative intensities of the NH (~3100 cm^{-1}) and C=O (~1700 cm^{-1}) stretching bands as well as the emergence of a band at 1620 cm^{-1}, which indicates the formation of a C=C or C=N group. Further characteristic bands of these products occur at 1235 and 774 cm^{-1}. Chierotti et al. [29] reported just recently that grinding of pure form II of BAc for 24 h with a ball mill results in the tri-hydroxyl tautomer, which is probably the least stable of the nine potential tautomeric forms of BAc. According to Slesarev and Popov [30] the keto–enol form is the most probable tautomer that can be formed in a protic environment, whereas lactim–lactam transformations are less favored. Nevertheless, our infrared experiments show clearly that the molecular structure of BAc changes on grinding with potassium bromide, which obviously provides (together with traces of water) the condition for a proton transfer and the formation of one (or more) stabilized tautomer(s). In contrast to polymorphic phase changes or desolvation reactions that can easily happen during the preparation of alkali halide discs, true mechanochemical reactions are less common. Examples for the occurrence of ion exchange reactions, complex formations and oxidations are summarized and discussed in a review by Fernandez-Bertran and Reguera [31]. These reactions concern mainly inorganic salts whereas reports for organic compounds are rather rare and limited to ion exchange reactions in salts or to neutral carboxylic acids. An example is the zwitterion formation in pyridinecarboxylic acids (nicotinic, picolinic and isonicotinic acid) [32]. However, the intriguing reaction observed in BAc provides a challenging task for further investigations (e.g. with solid-state NMR) which are beyond the object of the present study.

FT-Raman spectra (Fig. 7) also allow a clear distinction between the different forms. Particularly the C—H stretching vibrations close to 3000 cm^{-1}, the C=O bands around 1750 cm^{-1}, and the phonon vibrations in the far infrared region (<200 cm^{-1}) reflect their structural diversity. Some of the band maxima positions are listed in Table 1. The Raman data of form II are in good agreement with those reported in a study of de Oliveira et al. [33], who provide detailed assignments of the observable bands.

3.5. Powder X-ray diffraction (PXRD)

The experimental X-ray powder diffraction patterns are shown in Fig. 9 along with calculated patterns from single crystal structure for form II and the dihydrate. Experimental and calculated patterns match very well. The fact that the theoretical diffractogram of form II was calculated from a low temperature structure determination [12], whereas the experimental pattern was measured at room tem-

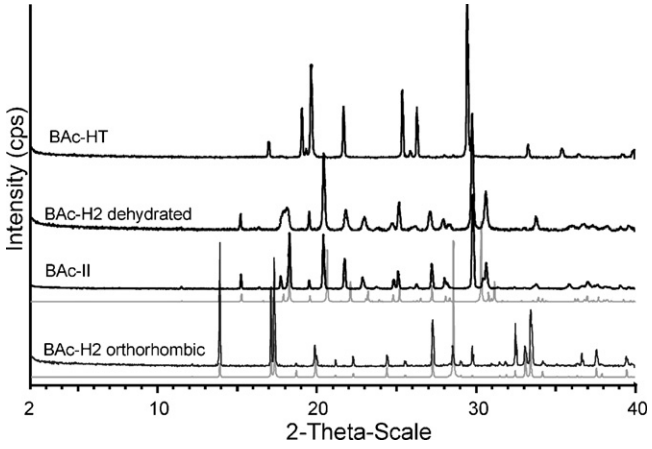

Fig. 9. Experimental PXRD diffractograms (black lines) of the HT-form (top) of barbituric acid, form II obtained by heating in DSC until 248 °C, and desolvation of BAc-H2 (middle) and the orthorhombic hydrate (bottom). The light grey patterns represent the theoretical diffractograms calculated from the crystal structures of the dihydrate (CSD ref. code: BARBAD, $T \approx 20$ °C) and form II (CSD ref. code BARBAC02, $T = -123$ °C).

perature, explains why some peaks in the calculated pattern are shifted relative to those in the experimental diffractogram of form II.

The powder pattern of BAc-H2 dehydrated at 0% RH shows broader reflections, which can be explained by particle size effects (formation of micro- to nanosized crystals of form II upon desolvation) and the formation of structural defects, which is common in such desolvation reactions. We also performed time resolved PXRD experiments at 30 °C and 31% RH to monitor the desolvation reaction of the dihydrate (see supplementary material). This experiment showed that the dehydration of the hydrate and the formation of form II occurs simultaneously and not via a distinct crystalline or a disordered intermediate state, thus confirms the conclusions derived from microscopic and thermoanalytical investigations (see above).

We have reproducibly obtained the pattern of the HT-form shown in Fig. 9, which however is different to the diffractogram reported by Roux et al. [15]. We have noticed that some of the reflections match with the reflections in a pattern that we obtained from a thermally decomposed product. Since some experimental details concerning the production and measurement conditions are missing in Roux's paper, we unfortunately cannot comment on the reasons for this discrepancy. The indexing of the HT-form indicated a monoclinic space group $P2_1/n$ with four formula units per unit cell and the lattice parameters $a = 9.293(4)$ Å, $b = 6.765(3)$ Å, $c = 8.185(5)$ Å, $\beta = 91.75(2)°$ ($V = 514.34(2)$ Å^3, $R_{wp} = 13.29$, $R_{exp} = 10.10$, $R_{Bragg} = 9.65$). The Le Bail fit and difference plot between calculated and experimental pattern is shown in Fig. S3 (supplementary material). As expected, this unit cell metric is not in accordance with Roux et al. [15] who found two triclinic ($P1$) cells. However, neither these nor our cell parameters match with one of the ab initio predicted structures of Lewis et al. [12].

3.6. Structural changes upon dehydration

A special structural feature of the dihydrate of BAc is the formation of perfectly planar layers [10,17]. These layers are essentially maintained upon the dehydration process to form II [12]. However, the crystal structure of form II shows two crystallographic independent molecules with slightly different conformations (an envelope and planar conformer) which are also slightly tilted out of plane. Because of this planar arrangement, it is rather straightforward to illustrate the structural differences of the two forms and

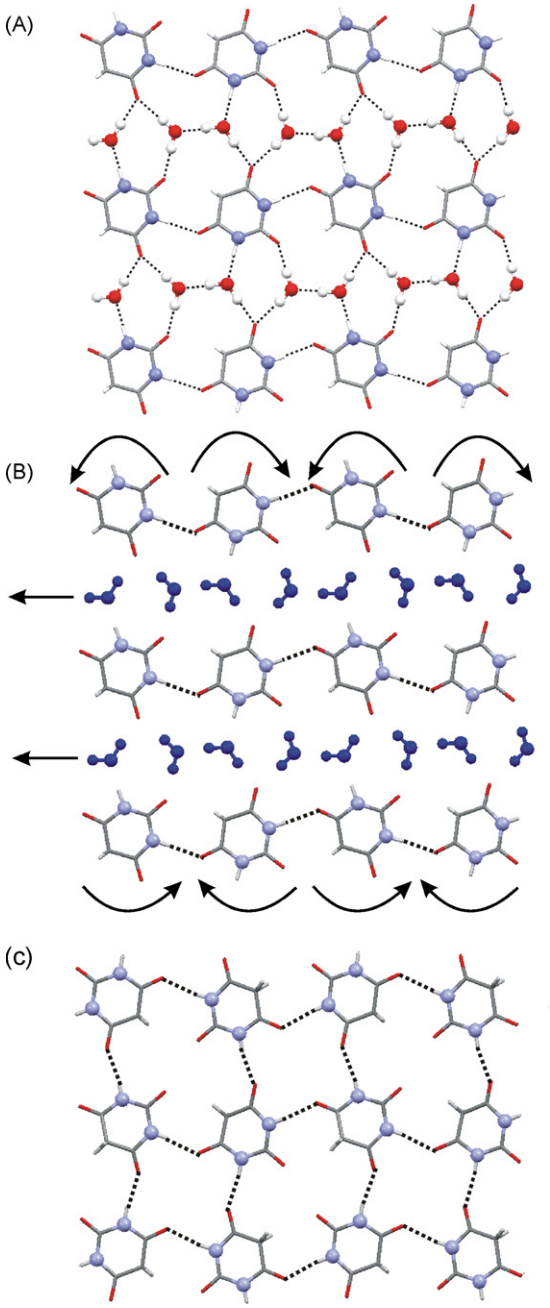

Fig. 10. Hydrogen bonding motif of barbituric acid (A) dihydrate, (B) probable changes during the dehydration process to form II, and (C) the dehydration product form II. Both structures are forming 2D sheets. CSD ref. codes: BARBAC (dihydrate, [10]) and BARBAC02 (form II, [12]).

to get an idea about the reorganization within the 2D layers after the water molecules are released. Fig. 10 shows the intermolecular connectivity patterns of barbituric acid BAc-H2 and form II, and the possible transformation mechanism. In form II the pyrimidine rings of barbituric acid are linked through four N—H···O hydrogen bonds generating 2D-sheets (Fig. 10-C), which propagate parallel to the b-axis, where the O(2) in form II is not involved in hydrogen bonding. In the dihydrate the BAc molecules form 2D-chains (Fig. 10A) linked by only one direct N—H···O hydrogen bond. These chains are connected via hydrogen bonds to the water molecules, which are also aligned in chains along the a-axis of this orthorhombic crystal. The release of water from the dihydrate is connected with a disruption of the four different hydrogen bonds between a BAc molecule and four water molecules (Fig. 10B). Once the space between the BAc

molecules is empty, an alternating twist of the molecules in every second chain and the breaking of the existing N—H···O hydrogen give the basic arrangement for the new connectivity (formation of three new H-bonds) in form II. As already pointed out by Braga et al. [14], the requirement of rather moderate structural changes is a plausible explanation for the unexceptional transformation of the BAc dihydrate to form II instead of form I which shows a quite different structure (hydrogen-bonded chains that pack in a herringbone motif (see refs. [11] and [14]).

4. Conclusions

So far six crystal forms of barbituric acid have been clearly identified, three polymorphs, two forms of the dihydrate and a dioxane solvate. Our studies confirm that form II is the thermodynamically stable form at 20 °C and the most important and relevant solid-state form of BAc. Even though the crystal structure of this polymorph has been determined quite recently [12] it is obvious that form II has been present since the first days of this popular compound. This becomes also clear when its moisture dependent stability is taken into consideration. We showed that the formation of the hydrate occurs at relative humidities of ≥80%, whereas the hydrate dehydrates to form II already at ≤50% RH. Thus, the hydrate is not very durable and transforms easily back to form II under usual storage conditions. We experienced that form I is rather unstable and quickly transforms to the stable form II in the mother liquor. A few DSC runs of mixtures of form I with form II showed an exothermic event at around 60 °C, which indicates a monotropic relationship between the two forms. The fact that Bolton [11] obtained right this metastable form as a single crystal, 40 years before the structure of the stable form II was published, represents a very typical "accident" (or serendipity?) in single crystal structure analysis. However, we can confirm the existence of the high-temperature form, which had been detected quite recently by Roux et al. [15]. This form invariably occurs on heating to about 13 K below its melting point. Thus, it is presumed that all melting points reported so far in the literature correspond to this HT-form and not form II. In other words, this HT-form has been produced frequently over the last 140 years albeit by accident and unrecognized. The two forms (II, HT) are enantiotropically related and due to its rather low kinetic stability, the HT-form transforms back to form II at ambient temperature. Furthermore, it should be mentioned that we could crystallize the dioxane solvate [16] (see Fig. S4 in the supplementary material). This solvate desolvates readily at ambient conditions to form II (proven by PXRD).

Thermal and moisture dependent desolvation studies on BAc-H2 show the typical behaviour of a stoichiometric hydrate that is unstable at lower water vapor pressures and exhibits limited water solubility. We have demonstrated that it is very useful to perform DSC experiments at different container conditions and combine this obtained information with microscopy studies in order to understand the desolvation process of a hydrate. Since the dihydrate transforms quantitatively to pure form II, it was also possible to determine the enthalpy of this reversible transformation process $\Delta_{trs}H_{II\text{-}H2}$ with DSC. A value of the same magnitude was calculated from the heat of solution differences of the BAc-H2 and form II (solution calorimetry measurements in water), and was also obtained by isothermal calorimetry using a controlled RH-perfusion unit.

A surprising observation was a tautomeric change that can be easily induced by grinding BAc together with potassium bromide. Therefore, published IR-spectra recorded from KBr-disc always show variable amounts of a tautomer besides the stable trioxo-form, depending on the mechanical treatment of the mixture.

This study provides a variety of new thermophysical data of BAc and demonstrates possible strategies of investigation for the solid-state forms and phenomena. Finally the chronology of discovery of new forms of this old compound points out how little we know about the solid-state properties of heavily used fine chemicals and that thermophysical data (even a simple melting point) are of limited value if not accompanied by a reference to a specific solid-state form.

Acknowledgement

The authors would like to thank Dr. Thomas Gelbrich for helpful discussions and constructive criticism.

Appendix A. Supplementary data

Supplementary data associated with this article can be found, in the online version, at doi:10.1016/j.tca.2008.12.001.

References

[1] D. Thetford, A.P. Chorlton, J. Hardman, Dyes Pigments 59 (2003) 185–191.
[2] A.V. Kulinich, N.A. Derevyanko, A.A. Ishchenko, Russ. J. Gen. Chem. 76 (9) (2006) 1441–1457.
[3] A. Slaczka, J. Lubczak, J. Appl. Polym. Sci. 106 (6) (2007) 4067–4074.
[4] M. Tishler, K. Pfister, R.D. Babson, K. Ladenburg, A.J. Fleming, J. Am. Chem. Soc. 69 (1947) 1487–1492.
[5] A. von Baeyer, Ann. Chem. Pharm. 127 (1863) 199–236.
[6] M.K. Carter, J. Chem. Educ. 28 (1951) 524–526.
[7] R. Hilfiker (Ed.), Polymorphism in the Pharmaceutical Industry, Wiley-VCH, Weinheim, 2006, pp. 211–233.
[8] J. Bernstein, Polymorphism in Molecular Crystals, Oxford Science Publications, Oxford, 2002.
[9] P. Erk, H. Hengelsberg, M.F. Haddow, R. van Gelder, CrystEngComm 6 (2004) 474–483.
[10] G.A. Jeffrey, S. Ghose, J.O. Warwicker, Acta Crystallogr. 14 (1961) 881–887.
[11] W. Bolton, Acta Crystallogr. B 16 (1963) 166–173.
[12] T.C. Lewis, D.A. Tocher, S.L. Price, Cryst. Growth Des. 4 (5) (2004) 979–987.
[13] T.C. Lewis, D.A. Tocher, S.L. Price, Cryst. Growth Des. 5 (3) (2005) 983–993.
[14] D. Braga, M. Cadoni, F. Grepioni, L. Maini, K. Rubini, Cryst. Eng. Comm. 8 (10) (2006) 756–763.
[15] M.V. Roux, M. Temprado, R. Notario, C. Foce-Foces, V.N. Emelýaneko, S.P. Verevkin, J. Phys. Chem. A 112 (2008) 7455–7465.
[16] S. Al-Saqqar, L.R. Falvello, T. Soler, J. Chem. Crystallogr. 34 (1) (2004) 61–65.
[17] G.S. Nichol, W. Clegg, Acta Crystallogr. B 61 (2005) 464–472.
[18] A. Berlin, M. Taylor, R.J. Robinson, Anal. Chim. Acta 24 (1961) 427–431.
[19] S.R. Byrn, R. Pfeiffer, J.G. Stowell, Solid-state Chemistry of Drugs, second ed., SSCI, Inc., West Lafayette, Indiana, 1999, p. 233.
[20] U.J. Griesser, A. Burger, Int. J. Pharm. 120 (1) (1995) 83–93.
[21] E. Suzuki, K. Shimomura, K. Sekiguchi, Chem. Pharm. Bull. 37 (2) (1989) 493–497.
[22] X'Pert HighScore Plus (PW3212), Release: Version 2.2c (c) PANalytical B.V. (2007).
[23] R. Shirley, The Crysfire 2002 System for Automatic Powder Indexing: User's Manual, The Lattice, England, 2002.
[24] J. Laugier, B. Bochu, Checkcell, INPG Grenoble, Saint Martin dïHères, France.
[25] G.A. Uriano, National Bureau of Standards Certificate. Standard Reference Material 1655, Potassium Chloride, KCl(cr) for Solution Calorimetry, Washington, DC, 1981.
[26] A. Burger, R. Ramberger, Mikrochim. Acta II (1979) 273–316.
[27] J.A. Riddick, W.B. Bunger, Organic Solvents. Physical Properties and Methods of Purification, fourth ed., Wiley-Interscience, New York, 1970.
[28] Y.-S. Kim, J.R. Mendez del Rio, R.W. Rousseau, J. Pharm. Sci. 94 (9) (2005) 1941–1948.
[29] M.R. Chierotti, R. Gobetto, L. Pellegrino, L. Milone, P. Venturello, Cryst. Growth Des. 8 (5) (2008) 1454–1457.
[30] V.I. Slesarev, A.S. Popov, Russ J. Gen. Chem. 69 (6) (1999) 986–995.
[31] J. Fernández-Bertrán, E. Reguera, Solid State Ionics 93 (1997) 139–146.
[32] L.D. Taylor, J. Org. Chem. 10 (1959) 1064.
[33] L.F.C. de Oliveira, P.S. Santos, J.C. Rubim, J. Raman Spectrosc. 22 (9) (1991) 485–488.